JOURNAL OF COMPUTATIONAL PHYSICS 69, 267–282 (1987)

The Liouville Theorem and Accurate Plasma Simulation

H. RALPH LEWIS, DANIEL C. BARNES,* AND KARL J. MELENDEZ

Los Alamos National Laboratory, Los Alamos, New Mexico 87545

Received July 31, 1985; revised March 21, 1986

The cold two-stream instability has been examined within the context of the one-dimensional Vlasov–Poisson model for three simulation methods. Two of the methods treat a continuum of particles; the third is the particle-in-cell method. The onset of noise in the simulations occurred near the time when the beams crossed or nearly crossed in the phase space, indicating a violation of Liousville's theorem or strong sensitivity of particle trajectories to initial conditions in the vicinity of the point of near crossing. Details of the underlying Hamiltonian structure of the particle dynamics appear to be important in achieving accurate plasma simulations. © 1987 Academic Press, Inc.

I. INTRODUCTION

Numerical simulation of collisionless plasmas by means of discrete-particle Lagrangian techniques is a useful tool in plasma physics. Rapid development of the subject began during the latter years of the 1960s and continued for five or six years. Following that, until several years ago, emphasis shifted from development of techniques to specific numerical applications. Although use of the science and art of numerical plasma simulation has contributed greatly to the present-day understanding and application of plasma physics, plasma simulation techniques still have shortcomings that prohibit application to some important and interesting problems.

During the early years, we sought better techniques for collisionless plasma simulation. However, our attempts to improve simulation techniques significantly were unsuccessful and we relinquished our efforts in 1973. During our work, we observed a correlation between the onset of noise in simulations and crossing or near crossing of particle trajectories in phase space. We are reporting on this observation now, despite the long delay, because it is relevant to some current ideas for improving plasma simulation methods by using Hamiltonian approximation methods for the particle trajectories. A discussion of one such idea is presented in Ref. [1].

Our work dealt exclusively with the one-dimensional, single-species Vlasov–Poisson system. Other numerical experiments, with various implementations of par-

* Present address: Science Applications International Corp., 206 Wild Basin Road, Austin, Tex. 78746.

0021-9991/87 $3.00

ticle-in-cell simulation, have indicated that modifying the method of solving the Poisson equation will not lead to a significant reduction of the observed noise in the solution that limits the class of problems which can be studied with the particle-in-cell method [2–4]. Particle-in-cell methods may be viewed as limiting cases of Lagrangian formulations based on a continuum of particles; the limit is that the continuum is replaced by a finite set of discrete particles. The notion of a continuum of particles underlies the Vlasov equation, and it can be argued on an a priori basis that the noise in particle-in-cell simulations is the result of replacing the continuum with a relatively small number of discrete particles. For that reason we tried certain approximation schemes that are based on a continuum of particles instead of discrete particles. In Lagrangian representations, the fundamental function that describes the particles is the particle position as a function of initial position, initial velocity and time. A particular approximation of that function was proposed by Lewis [5] for the case in which there were initially N cold beams. For each initial velocity, the particle position is approximated by the initial position plus a truncated Fourier series in the initial position with time-dependent coefficients; and the electric potential is approximated by a Fourier series in position. This results in a system of ordinary differential equations in time whose coefficients involve complicated integrals over initial position and velocity. We tried this scheme with the result that too much computer time and storage were required in order to obtain a numerical solution over a sufficiently large number of plasma periods.

In order to test the value of expanding the particle position in a Fourier series in initial position, we modified this scheme in a way that allowed numerical results to be obtained much more easily. The most important modification was to solve the Poisson equation by a modified particle-in-cell method, while retaining the Fourier series representation of the particle position. Computations with the revised scheme demonstrated that it was not preferable to particle-in-cell methods; noise occurred with this scheme just as noise occurs in particle-in-cell solutions. However, an interesting correlation with the onset of the noise was observed in these computations: the onset of noise was accompanied by an obvious breakdown of measure preservation in phase space as manifested by actual crossing of phase-space trajectories. Crossing or near crossing turned out to be central to our observation of noise in all of our computations, including a variety of particle-in-cell simulations.

Another continuum method which we tried was characterized by a piecewise linear approximation of particle position as a function of initial position and by an exact, analytic solution of the Poisson equation. Again noise occurred whose onset was accompanied by crossing of phase-space trajectories.

We also performed particle-in-cell computations in our search for the basic cause of the noise in the electric field. The Poisson equation was solved with the standard linear interpolation procedure for the charge density. For moving the particles we tried a standard leapfrog algorithm as well as a fourth-order Runge–Kutta method. The number of particles, the number of cells and the time step were varied. We

observed that the onset of noise in these calculations was accompanied by conditions which were at least very close to crossing of trajectories in phase space. Even if the trajectories did not actually cross, there was a strong sensitivity of trajectories to initial conditions in the vicinity of the place where they nearly crossed. The only thing which we found effective in delaying crossing or near-crossing of trajectories, and the concommitant onset of noise, was improvement of the accuracy of integrating the particle equations of motion, either by using the fourth-order Runge–Kutta scheme instead of the leapfrog algorithm, or by decreasing the time step.

We believe that we have compelling evidence that the onset of noise in all methods of Lagrangian numerical simulation of the Vlasov–Poisson system is correlated with inaccuracies in the particle trajectories in vicinities where there is strong sensitivity to initial conditions. This effect has also been discussed by Dilber, Walsh and Denavit in terms of Kolmogorov–Sinai entropy [6]. We suggest that a major advance in techniques of numerical plasma simulation could be achieved by developing a practical simulation method in which certain features of the underlying Hamiltonian particle dynamics were treated more accurately. A practical technique for representing the particle data by a continuum in such a way that phase-space measure be preserved locally may lead to such an advance. In this way, the already powerful tool of numerical plasma simulation would become even more valuable.

In Section II we review the Lagrangian formulation of the Vlasov–Poisson system. We describe our various approximation schemes in Section III. Numerical results and our conclusions are presented in Sections IV and V, respectively.

II. Lagrangian Formulation

We consider the simplest Vlasov–Maxwell system. All quantities are assumed to vary spatially in only one dimension, x, and their dependence on x is assumed to be periodic with period L. In addition, the plasma is assumed to be unmagnetized so that only electrostatic interactions need be considered.

The equations describing such a system are the one-dimensional Vlasov equation

$$\frac{\partial f}{\partial t} + v \frac{\partial f}{\partial x} + \frac{q}{m} E(x, t) \frac{\partial f}{\partial v} = 0, \tag{1}$$

with initial data

$$f(x, v, 0) = f_0(x, v), \tag{2}$$

and the Poisson equation

$$\frac{\partial^2 \phi}{\partial x^2} = 4\pi q \left[n_0 - \int f(x, v, t)\, dv \right], \tag{3}$$

where $E(x, t) = -\partial/\partial x\, \phi(x, t), -n_0 q$ is a uniform neutralizing background charge density and ϕ satisfies the boundary condition

$$\phi(0, t) = \phi(L, t) \Leftrightarrow \int_0^L E(x, t)\, dx = 0. \tag{4}$$

The approximation schemes that we consider here as well as all conventional plasma simulation methods are Lagrangian in nature. That is, the solution of the characteristic equations of (1), which are the equations of motion of a particle of mass m and charge q moving in the electric field $E(x, t)$, is approximated numerically for some set of initial conditions. The particle distribution function, $f(x, v, t)$, is constructed from the set of particle trajectories and the electric potential is determined self-consistently by solving the Poisson equation (3). Let $X(x', v', t)$ and $V(x', v', t)$ be, respectively, the position and velocity of a particle at time t whose position and velocity at time 0 are x' and v', respectively. These functions are the solution of the particle equations of motion

$$\dot{X}(x', v', t) = V(x', v', t), \qquad \dot{V}(x', v', t) = \frac{q}{m} E[X(x', v', t), t] \tag{5}$$

with the initial data

$$X(x', v', 0) = x', \qquad V(x', v', 0) = v', \tag{6}$$

where a dot over a quantity denotes partial differentiation with respect to t. The transformation from (x', v') to (x, v) given by

$$x = X(x', v', t), \qquad v = V(x', v', t) \tag{7}$$

can always be inverted to express x' and v' in terms of x, v and t. We write the inverse as

$$x' = X_0(x, v, t), \qquad v' = V_0(x, v, t). \tag{8}$$

The solution of the Vlasov equation (1) with the initial data (2) can be expressed in terms of the functions X_0 and V_0 as

$$f(x, v, t) = f_0[X_0(x, v, t), V_0(x, v, t)]. \tag{9}$$

The Vlasov–Maxwell equations for a collisionless plasma can always be considered as a complete Hamiltonian system for the electromagnetic potentials and the functions that give the position of a particle moving in the electromagnetic field as a function of initial position, initial velocity and time [5]. For the Vlasov–

Poisson system that we are considering here, but allowing the possibility that the system be nonperiodic, the Lagrangian is

$$L = \int dx' \int dv' f_0(x', v') \left\{ \frac{1}{2} m\dot{X}(x', v', t)^2 - q\phi[X(x', v', t), t] \right\} + \int dx \left\{ \frac{1}{8\pi} \left(\frac{\partial \phi}{\partial x} \right)^2 + n_0 q \phi(x, t) \right\}. \tag{10}$$

In general, the integrations over x' and v' extend over the full ranges of initial position and velocity; the integration over x extends over the domain of definition of the problem. For a periodic system, the integrations over x' and x may be restricted to a single period. Appropriate boundary conditions on the potential must be specified at the endpoints.

It is possible to express $\phi(x, t)$ explicitly in terms of $X(x', v', t)$ and $f_0(x', v')$. For an aperiodic system, the result is

$$\phi(x, t) = \phi_0 + \phi_1 x + \frac{4\pi q}{L} \int dx' \, dv' f_0(x', v') \left\{ \frac{1}{2} [x - X(x', v', t)]^2 - \frac{L}{2} |x - X(x', v', t)| \right\}, \tag{11}$$

where ϕ_0 and ϕ_1 are constants that are determined by the boundary conditions and L is the length of the system. That (11) solves the Poisson equation depends on the formula

$$\frac{d^2}{dy^2} \frac{1}{2} |y| = \delta(y). \tag{12}$$

For a periodic system the result is

$$\phi(x, t) = \phi_0 + \frac{4\pi q}{L} \int dx' \, dv' f_0(x', v') \times \left\{ \frac{1}{2} [[x - X(x', v', t)]_{\mathrm{mod}\, L}]^2 - \frac{L}{2} [x - X(x', v', t)]_{\mathrm{mod}\, L} \right\}, \tag{13}$$

where ϕ_0 is a constant, L is the periodicity length of the system and the integral over x' is from 0 to L. The function $y_{\mathrm{mod}\, L}$ is a modulo function defined by

$$y_{\mathrm{mod}\, L} = y - nL, \tag{14}$$

where n is an integer defined by

$$nL \leqslant y < (n + 1) L. \tag{14a}$$

This function is clearly periodic with period L and satisfies the identity

$$\frac{1}{2}[y_{\mathrm{mod}\,L}]^2-\frac{L}{2}\,y_{\mathrm{mod}\,L}=\frac{1}{2}y^2-\frac{L}{2}|y|, \qquad -L\leqslant y\leqslant L. \tag{15}$$

Therefore, the formula

$$\frac{d^2}{dy^2}\left\{\frac{1}{2}[y_{\mathrm{mod}\,L}]^2-\frac{L}{2}\,y_{\mathrm{mod}\,L}\right\}=1-L\,\delta_L(y) \tag{16}$$

holds, where

$$\delta_L(y)=\delta(y) \qquad \text{for} \quad -\frac{L}{2}\leqslant y\leqslant\frac{L}{2} \tag{17}$$

and is periodically extended for all other values of y. That (13) solves the Poisson equation is a result of formula (16).

The particle equations of motion (5) can be derived from a particle Lagrangian, L_p, which is that part of the complete Lagrangian (10) that depends on the mapping function X. By substituting the potential given by (13) into L_p, we express L_p for the periodic case in terms of the mapping function alone, without explicit reference to the potential:

$$\begin{aligned}L_p=&\frac{m}{2}\int dx'\,dv'\,f_0(x',v')\,\dot{X}(x',v',t)^2-q\phi_0\int dx'\,dv'\,f_0(x',v')\\&-\frac{2\pi q^2}{L}\int dx'\,dv'\,dx''\,dv''\,f_0(x',v')\,f_0(x'',v'')\\&\times\{[[X(x',v',t)-X(x'',v'',t)]_{\mathrm{mod}\,L}]^2-L[X(x',v',t)-X(x'',v'',t)]_{\mathrm{mod}\,L}\}.\end{aligned} \tag{18}$$

The last term can be evaluated as

$$\begin{aligned}&2\pi q^2\int dx'\,dv'\,dx''\,dv''\,f_0(x',v')\,f_0(x'',v'')[X(x',v',t)-X(x'',v'',t)]_{\mathrm{mod}\,L}\\&\quad=\pi q^2\int dx'\,dv'\,dx''\,dv''\,f_0(x',v')\,f_0(x'',v'')\\&\qquad\times\{[X(x',v',t)-X(x'',v'',t)]_{\mathrm{mod}\,L}+[X(x'',v'',t)-X(x',v',t)]_{\mathrm{mod}\,L}\}\\&\quad=\pi q^2L\int dx'\,dv'\,dx''\,dv''\,f_0(x',v')\,f_0(x'',v''),\end{aligned} \tag{19}$$

where we have used the identity

$$(-y)_{\mathrm{mod}\,L}+(y)_{\mathrm{mod}\,L}=L. \tag{20}$$

Neither this term in L_p nor the term proportional to ϕ_0 depends on the mapping function X. Therefore, both terms can be deleted from L_p to give

$$L_p = \frac{m}{2} \int dx'\, dv'\, f_0(x', v')\, \dot{X}(x', v', t)^2 \tag{21}$$

$$-\frac{2\pi q^2}{L} \int dx'\, dv'\, dx''\, dv''\, f_0(x', v')\, f_0(x'', v'')[[X(x', v', t) - X(x'', v'', t)]_{\mathrm{mod}\, L}]^2.$$

III. Approximation Schemes

We have examined the cold two-stream instability with three approximation schemes. Two of them, which we denote by Fourier–PIC and piecewise linear, describe a continuum of particles with a finite number of time-dependent parameters. The third scheme is a PIC (particle-in-cell) method. In our application of the PIC scheme, which describes a finite number of discrete particles, we tried two algorithms for advancing the particles in time.

The Fourier–PIC scheme is a modification of a scheme proposed by Lewis and Melendez. They represented the mapping function $X(x', v', t)$ for each beam as x' plus a truncated Fourier series in x'; and they represented the electric potential as a truncated Fourier series in position x. The equations for advancing the coefficients of these Fourier series in time where derived from Hamilton's principle. As described in Section V of Ref. [5], these equations involve time-dependent quantities that are Fourier coefficients in the Fourier series expansion of a complex exponential of a truncated Fourier series. As the two-stream instability develops, these coefficients become increasingly difficult to evaluate and a special numerical method was developed for their evaluation [7]. Sufficiently far in the evolution of the instability, even this method is ineffective, but there was evidence that the integrals could be evaluated effectively by the method of stationary phase from that time on. A computer code for evaluation by the method of stationary phase was written. However, the result was that the method described in Ref. [7] for evaluating the integrals was not effective for a long enough time such that the method of stationary phase would be applicable thereafter. Because of this intermediate period during the evolution, when the task of evaluating certain time-dependent quantities in the differential equations was insurmountable, the approximation scheme proposed by Lewis and Melendez was abandoned as being impractical.

The Fourier–PIC scheme used here retains the representation of the mapping function $X(x', v', t)$ for each beam as x' plus a truncated Fourier series in x',

$$X(x', \pm V, t) = x' \pm V \left\{ \delta_0^{(\pm)}(t) + \sum_{n=1}^{N} \left[\gamma_n^{(\pm)}(t) \sin \frac{2\pi n x'}{L} + \delta_n^{(\pm)}(t) \cos \frac{2\pi n x'}{L} \right] \right\}, \tag{22}$$

where the initial conditions are

$$\gamma_n^{(\pm)}(0) = \delta_n^{(\pm)}(0) = 0, \tag{23a}$$

$$\dot{\gamma}_n^{(\pm)}(0) = \dot{\delta}_n^{(\pm)}(0) = 0, \qquad n \neq 0, \tag{23b}$$

$$\dot{\delta}_0^{(\pm)}(0) = 1. \tag{23c}$$

This ansatz describes two continuous beams, whose initial velocities are $\pm V$, in terms of the $2(2N+1)$ time-dependent parameters $\gamma_n^{(\pm)}(t)$ and $\delta_n^{(\pm)}(t)$. Equations for advancing these time-dependent parameters can be derived from the variation of the action associated with the Lagrangian (10). They are the same as those obtained by applying a Galerkin method to the equation of motion for each beam,

$$X(x', \pm V, t) = \frac{q}{m} E[x', \pm V, t), t]. \tag{24}$$

Specifically, the equation of motion for each beam is multiplied by the spatial initial distribution function for that beam and by one of the $(2N+1)$ expansion functions

$$1, \qquad \sin \frac{2\pi n x'}{L}, \qquad \cos \frac{2\pi n x'}{L};$$

then the resulting equation is integrated with respect to x' from 0 to L. The $2(2N+1)$ equations obtained by repeating this for each beam and for each expansion function are a system of second-order differential equations in time.

In contrast to the method of Lewis and Melendez (Section V of Ref. [5]), we determine the electric field for the Fourier–PIC scheme by a particle-in-cell method [8, 9, 5]. A set of equally spaced points in initial position is chosen for each beam and the positions of the corresponding particles are calculated at time t from (22). The charge density at time t is then calculated on a spatial mesh according to a standard PIC method with a linear weighting for the assignment of the charge of a particle to neighboring mesh points. The potential is determined by solving a finite-difference approximation to Poisson's equation with that charge density. In this way, evaluation of the very difficult integrals confronted by Lewis and Melendez is avoided and the computation time for determining the electric field is proportional to the size of the spatial mesh on which Poisson's equation is solved. The connection of this formulation to the Poisson equation obtained from the Lagrangian (10) is the following. A piecewise linear expansion of the potential ϕ on a regular mesh in x gives an integro-difference equation with the same difference operator that occurs in the finite-difference approximation. If the integral over the initial phase space is approximated by Euler's rule, then the Fourier–PIC approximation for Poisson's equation is obtained.

The piecewise linear scheme was conceived as an alternative to the method of Lewis and Melendez that perhaps would be practical. Like the method of Lewis

and Melendez, the piecewise linear scheme is completely Hamiltonian. The ansatz used in the piecewise linear scheme for the mapping function $X(x', v', t)$ is

$$X(x', \pm V, t) = x' + \sum_{n=1}^{N} a_n^{(\pm)}(t)\, g_n(x'), \tag{25}$$

where the functions $g_n(x')$ are a local basis for linear splines ("tent functions") with fixed nodes. The electric potential is represented exactly as an infinite Fourier series,

$$\phi(x, t) = \sum_{n=-\infty}^{\infty} \alpha_n(t) \frac{1}{\sqrt{2\pi}} e^{inx}. \tag{26}$$

The initial distribution function for each beam was chosen to be a piecewise linear function of position.

The equations for the time-dependent parameters $a_n^{(\pm)}(t)$ and $\alpha_n(t)$ that are required by Hamilton's principle [5] for the piecewise linear scheme involve only integrals that can be performed analytically. The equations for the coefficients $\alpha_n(t)$ can be solved analytically, in analogy with (13), and the equations for the coefficients $a_n^{(\pm)}(t)$ can then be written without explicit reference to the potential, in analogy with (21). In order to achieve this, it is convenient to use the formula

$$\sum_{n \neq 0} \frac{1}{n^2} e^{inx} = \frac{1}{2} (x_{\mathrm{mod}\, 2\pi})^2 - \pi (x_{\mathrm{mod}\, 2\pi}) + \frac{\pi^2}{3}. \tag{27}$$

Although the integrals in the variational equations for the $a_n^{(\pm)}(t)$ can be carried out explicitly, there are many integrals and the equations are very complex. Because the potential has been determined exactly for any given form of the mapping function $X(x', v', t)$, every point in the plasma is explicitly in interaction with every other point. This is reflected in the fact that the computation time for solving the variational equations is proportional to the square of the number of piecewise linear basis functions used for representing the mapping functions for the two beams. Also, there are serious problems in evaluating certain quantities in the variational equations precisely enough when the slope of the mapping function for a beam is the same in neighboring cells.

A version of the piecewise linear scheme was also worked out in which the locations of the nodes for the mapping functions were allowed to vary in time. The dynamical equations for the complete set of variables, consisting of the amplitudes $a_n^{(\pm)}(t)$ and the locations, were derived from Hamilton's principle. However, the equations appeared to allow the nodes to move past one another, which must not be tolerated because the mapping functions must be single-valued. Therefore, the idea of variable nodes was abandoned in favor of (25).

Our third approximation scheme was a PIC method with standard linear weighting for assigning particle charge to neighboring mesh points [8, 9, 5]. We used two algorithms for advancing the particles. One was the usual leapfrog algorithm; the other was a fourth-order Runge–Kutta scheme.

IV. Numerical Results

The various approximation schemes described in Section III have been implemented and applied to one-dimensional, electrostatic plasma simulation. The simulation results presented in this section were all obtained for the same cold two-stream instability problem. The initial plasma was two cold, counter-streaming electron beams whose velocities are $\pm V$. The speed V is given by

$$\frac{V}{L\omega_p} = \frac{0.75}{2\pi}, \tag{28}$$

where L is the periodicity length of the system, $\omega_p^2 = 4\pi n_0 q^2/m$, and n_0 is the equilibrium plasma number density. If we define a Debye length in terms of V by

$$\lambda_D = \frac{V}{\omega_p}, \tag{29}$$

then the periodicity length is related to the Debye length by

$$L = \frac{2\pi}{0.75}\lambda_D. \tag{30}$$

The condition for instability of a density perturbation whose spatial variation is proportional to $\exp[i(2\pi\kappa x/L)]$ is

$$\frac{2\pi\kappa V}{L} < \omega_p. \tag{31}$$

Therefore, only a perturbation with the longest wavelength allowed in the system ($\kappa = 1$) was unstable in our simulations. For the Fourier–PIC and PIC simulations, 64 cells were used for Poisson's equation. A range of time steps was used, a typical time step being given by $\omega_p \delta t/(2\pi) = 0.04$. For the PIC simulations, the usual random initial loading of particles was modified to be regular in velocity space in order to achieve two completely cold beams initially.

Results with the Fourier-PIC scheme are shown in Figs. 1–3. The mapping function for one beam is shown in Fig. 1a at a time just after the maximum in the electric field energy has been reached. The phase-space plot at the same time for both beams is shown in Fig. 1b. The points plotted correspond to a set of particles in each beam that were equally spaced initially. Note that the two beams have nearly crossed in the phase space. The mapping function and phase-space plot are shown at a slightly later time in Figs. 2a and b; and they are shown at a still later time in Figs. 3a and b. In Fig. 2b the two beams have actually crossed and in Fig. 3b many crossings have occurred. As is illustrated in Fig. 1a, the mapping function becomes quite steep just prior to the first crossing of the beams. Just after the crossing, as illustrated in Fig. 2a, short wavelength oscillations develop near the

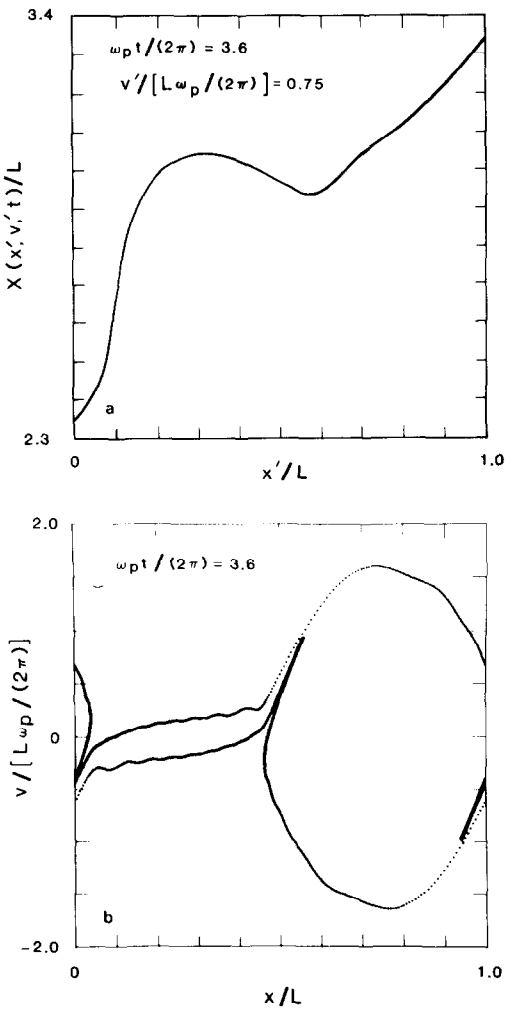

FIG. 1. (a) Fourier–PIC mapping function for one beam at $\omega_p t/(2\pi) = 3.6$. (b) Fourier–PIC phase-space plot at $\omega_p t/(2\pi) = 3.6$.

steep gradient. Further spreading of the oscillations and additional steepening, illustrated in Fig. 3a, then lead to the complex phase-space plot in Fig. 3b, which is characterized by multiple crossings of the beams.

When the two beams cross, the Jacobian of the phase-space map from (x', v') to (x, v) defined by (7) is no longer constant as required by Liouville's theorem. In the Fourier–PIC simulations, as well as with the piecewise linear and PIC simulations, we always observed a remarkable correlation between the first obvious breakdown of the Liouville theorem, as indicated by the first crossing or very near crossing of the beams, and the onset of noise in the simulation. With the Fourier–PIC and

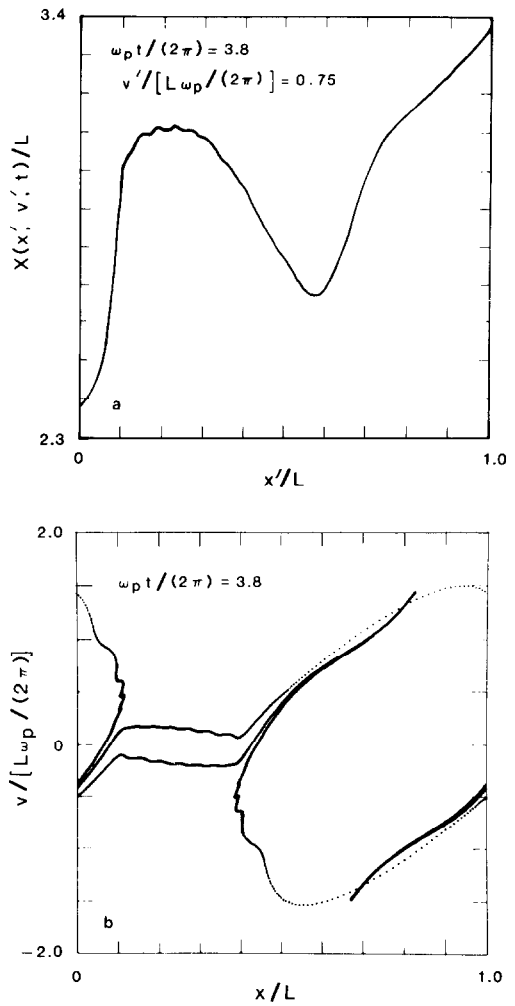

FIG. 2. (a) Fourier–PIC mapping function for one beam at $\omega_p t/(2\pi) = 3.8$. (b) Fourier–PIC phase-space plot at $\omega_p t/(2\pi) = 3.8$.

piecewise linear schemes, the beams always evolve as continuous curves in the phase space because the mapping functions are constrained to be continuous functions of x'. With those schemes, crossing was always observed to occur, no matter how many harmonics or nodes were used for representing the mapping functions. With the PIC scheme, each beam is represented by a finite number of discrete particles. After the beams very nearly crossed in PIC simulations, the particles in the vicinity of the crossing became disordered and the identities of the separate beams were lost. We denote by t_c the time at which the beams first cross or very nearly cross. The value of t_c was insensitive to the time step δt or to the other

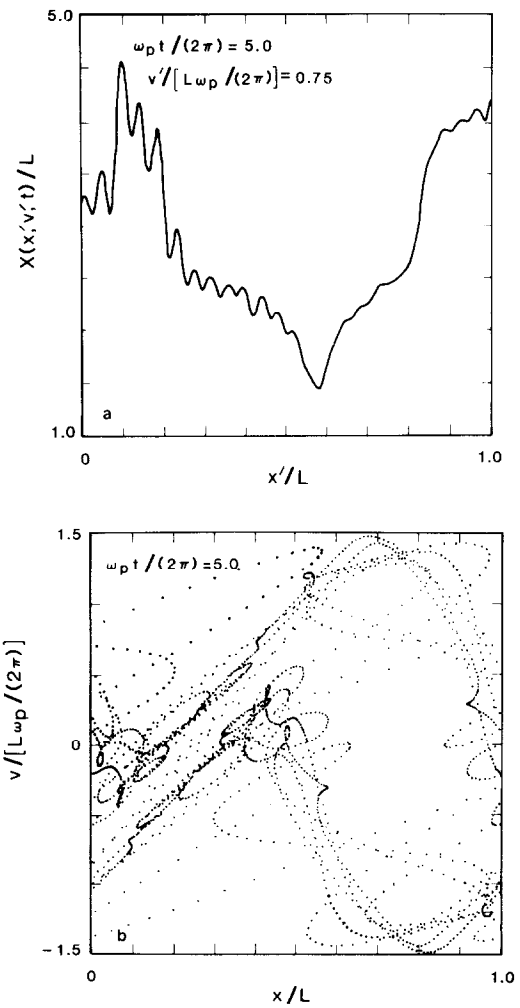

FIG. 3. (a) Fourier–PIC mapping function for one beam at $\omega_p t/(2\pi) = 5.0$. (b) Fourier–PIC phase-space plot at $\omega_p t/(2\pi) = 5.0$.

numerical parameters chosen for computing the mapping function: the number of Fourier harmonics in a Fourier–PIC simulation, the number of nodes in a piecewise linear simulation, or the number of particles in a PIC simulation. However, in all of the simulations, we observed noise after the time t_c, but not before. By this we mean the following. Suppose we have two simulations of the same problem with the same approximation scheme, but with different numerical parameters. The values of t_c for the two simulations will generally be different, but the simulations will be in good agreement for times earlier than the smaller of the two values. For later times, there will be significant differences. We call those dif-

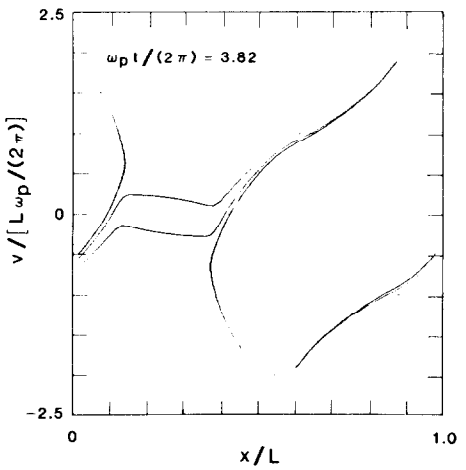

FIG. 4. PIC phase-space plot at $\omega_p t/(2\pi) = 3.82$.

ferences noise. The onset of noise was clearly evident in graphs of the electric field energy *versus* time. We give an example of that in connection with our discussion of PIC simulations below.

Results of simulations with the piecewise linear scheme were quite similar to the results with the Fourier–PIC scheme. Using equally spaced nodes, we found that the beams crossed in the phase space shortly after the peak in the electric field energy. The onset of noise occurred at approximately the time t_c.

Having observed with the Fourier–PIC and piecewise linear simulations that the onset of noise occurred very near the time t_c, we developed the PIC code in order to confirm this result with another method. As stated earlier, the results with the

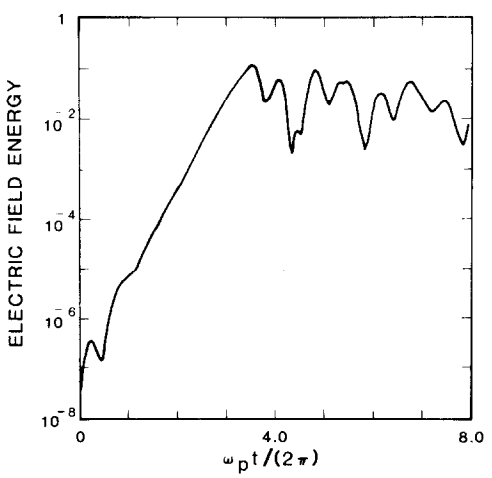

FIG. 5. PIC electric field energy history at $\omega_p \delta t/(2\pi) = 0.04$.

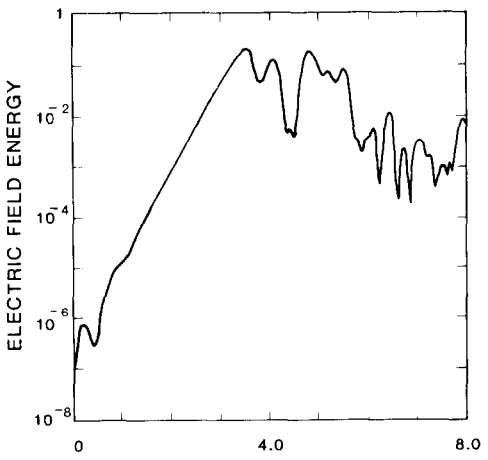

FIG. 6. PIC electric field energy history at $\omega_p \delta t/(2\pi) = 0.02$.

PIC code were very similar to the results with the other two schemes. We used two algorithms for advancing the particles with the PIC method. One was the standard leapfrog algorithm; the other was a fourth-order Runge–Kutta algorithm. The leapfrog algorithm is exactly measure-preserving. Therefore, trajectories would never actually cross in PIC simulations with the leapfrog algorithm, but they did nearly cross. With the two algorithms for time advancement with the PIC method, we studied the dependence of the results on the accuracy with which the particle equations of motion were integrated. We used values of $\omega_p \delta t/(2\pi)$ as small as 0.004. Although the value of t_c did increase as the equations of motion were integrated more accurately, it was rather insensitive to the accuracy.

In Fig. 4 is a phase-space plot from a PIC simulation at a time comparable to the Fourier–PIC plot in Fig. 2b. The beams have very nearly corssed. Shortly thereafter, the particles in the vicinity of the crossings became disordered and the identities of the beams were lost. In Figs. 5 and 6 are shown the electric field energy as a function of time from PIC simulations with two different time steps. In Fig. 5 the value of $\omega_p \delta t/(2\pi)$ is 0.04; in Fig. 6 the value is 0.02. The graphs differ markedly after the time t_c, which occurs shortly after the initial peak in the energy.

Because the onset of noise in our simulations was so strongly correlated with crossing or near crossing of the beams in the phase space, we believe that the noise is a result of inaccurate representation of details of the underlying Hamiltonian particle dynamics.

V. CONCLUSIONS

It would appear that details of the underlying Hamiltonian structure of the particle dynamics in plasma simulations is important for achieving accurate solutions of the initial-value problem. In our simulations, after a time when the beams

crossed or nearly crossed, representing a violation of Liouville's theorem or a strong sensitivity to initial conditions, the details of a simulation were no longer precise and the simulation could only be trusted on a statistical basis. In order to avoid these difficulties it would probably be necessary to find a computational method that treated certain features of the particle dynamics accurately. Some recent work in this direction has been carried out by Menyuk [1]. Also, recent work by Lewis, Leach and Goedert on invariants for time-dependent potentials may be relevant to this problem [10–12].

The science and art of numerical plasma simulation is a powerful tool in plasma physics. However, its applicablity would be even greater if a practical computational method were found which reliably reduced the noise in the gross physical quantities of interest.

Acknowledgments

One of us (H.R.L.) thanks Raymond C. Mjolsness for discussions concerning the formulation with a piecewise linear representation of $X(x', v', t)$ and he thanks Ivan Cherry for performing the large amount of computer programming associated with the numerical implementation of that formulation.

References

1. C. R. Menyuk, *Physica D* **11**, 109 (1984).
2. H. R. Lewis, A. Sykes, and J. A. Wesson, *J. Comput. Phys.* **10**, 85 (1972).
3. D. I. Brown, S. J. Gitomer, and H. R. Lewis, *J. Comput. Phys.* **14**, 193 (1974).
4. H. R. Lewis and C. W. Nielson, *J. Comput. Phys.* **17**, 1 (1975).
5. H. R. Lewis, *Methods in Computational Physics*, Vol. 9 (Academic Press, New York, 1970), pp. 307–338.
6. I. Dilber, J. M. Walsh, and J. Denavit, *J. Comput. Phys.* **52**, 545 (1983).
7. J. D. Thomas, H. R. Lewis, and K. J. Melendez, *J. Comput. Phys.* **12**, 462 (1973).
8. R. L. Morse, *Methods in Computational Physics*, Vol. 9 (Academic Press, New York, 1970), pp. 213–239.
9. C. K. Birdsall, A. B. Langdon, and H. Okuda, *Methods in Computational Physics*, Vol. 9 (Academic Press, New York, 1970), pp. 241–258.
10. H. R. Lewis and P. G. L. Leach, *Ann. Phys.* **164**, 47 (1985).
11. J. Goedert and H. R. Lewis, Rational functions of momentum as invariants for one-dimensional, time-dependent potentials: Basic theory, *J. Math. Phys.*, to appear.
12. H. R. Lewis and J. Goedert, Rational functions of momentum as invariants for one-dimensional, time-dependent potentials: Two- and three-resonance cases, *J. Math. Phys.*, to appear.